View Online

Superconducting $TaS_{2-x}I_y$ hierarchical nanostructures†

Xing-Cai Wu,* You-Rong Tao, Qi-Xiu Gao, Chang-Jie Mao and Jun-Jie Zhu

Received (in Cambridge, UK) 13th March 2009, Accepted 18th May 2009
First published as an Advance Article on the web 9th June 2009
DOI: 10.1039/b905168f

Iodine-doped TaS_2 hierarchical nanostructures, for which nanorod arrays are vertically grown on the edge of nanosheets, were prepared and showed superconductivity below 5 K.

Published on 09 June 2009 on http://pubs.rsc.org | doi:10.1039/B905168F
Downloaded by Nanjing University on 18 September 2010

Hierarchical assembly of nanoscale building blocks including nanocrystals, nanowires, and nanotubes is a crucial step toward realization of functional nanosystems.[1] Therefore, extensive efforts have been focused on integration of one-dimensional nanostructures or quantum dots into two/three-dimensional superstructures or much more complex functional architectures such as comb-like,[2] multipod-like,[3,4] and tree-like nanowires,[5,6] hyperbranched nanowire networks,[7–9] and hierarchical structured nanohelices.[10] Recently a series of chiral branched lead chalcogenide nanowires have been synthesized by chemical vapor deposition, and it was pointed out that the chiral branched structures open up new opportunities for tailoring the properties of nanomaterials.[11,12]

Tantalum disulfide (TaS_2) is an inorganic conductor with a layered structure, and displays a number of polytypes with a tantalum atom either in trigonal prismatic or octahedral coordination.[13] There are four principal polytypes: 1T-, 2H-, 3R- and 6R-TaS_2.[14] The layered structures enable extensive chemical intercalation, which are combined with the inherent superconductivity of both the parent compound and its intercalated derivatives.[15] A few TaS_2 nanostructures such as nanotubes,[16] nanoparticles,[17] and nanobelts,[18,19] have been prepared, but construction of complex nanosystems is still a challenge. Here we report a facile chemical-vapor-transport (CVT) technique using iodine as transport agent for the fabrication of a new $TaS_{2-x}I_y$ ($0 \leq x < 1$, $0 < y < 1$) architectures in which $TaS_{2-x}I_y$ nanorod arrays are vertically grown on the edges of $TaS_{2-x}I_y$ nanosheets.

In the experiment, tantalum (Ta) foils (99.9%) and sulfur (S) powder (99.5%) were used. Three pieces of Ta foils with size of *ca.* 0.2 × 5 × 10 mm (total weight: 650.1 mg; 3.59 mmol), S powder (11.5 mg; 0.359 mmol), and iodine powder (0.0, 30, 60 or 120 mg) were sealed in a quartz ampoule (Φ 6 × 13 mm) under a vacuum (*ca.* 10^{-2} Pa). The Ta foils were adjusted at the center of the ampoule. Then the ampoule was placed at the center of a conventional horizontal furnace (Φ 4 × 32 cm) with a temperature gradient of *ca.* 10 K cm^{-1} from center to end. The furnace was heated to 750 °C at rate of 12 °C min^{-1}, and kept at this temperature for 6 h. Then the furnace was cooled to room temperature, and the ampoule was opened and evacuated for 1 h to remove superfluous iodine. Finally the products were separated from the Ta foils for characterization. The products prepared with 0.0, 30, 60, and 120 mg of iodine were denoted as samples 1–4, respectively.

The products scraped from Ta foils were examined by a Shimadzu XRD-6000 X-ray diffractometer (XRD) with graphite-monochromatized Cu-Kα radiation and a JEOL model JEM-2100 high-resolution electron microscope (HRTEM) with a selected area electron diffraction (SAED) attachment. The morphologies were characterized by a S3400 scanning electron microscope (SEM) with energy-dispersive X-ray spectrometer (EDX; accuracy: 1%).

As shown in Fig. 1(a) and (b), samples 1 and 2 adopt the 3R-TaS_2 structure (*R*3*m*; a = 3.31 and c = 17.83 Å).[19] Sample 3 is shown to coexist of 2H- and 3R-TaS_2 structures, with the main phase being 2H-TaS_2 ($P6_3/mmc$; a = 3.31 and c = 12.58 Å; the parameters are close to those of standard card (ICDD PDF: 80–0685), shown in Fig. 1(c). Sample 4 has the 2H-TaS_2 structure (Fig. 1(d)).

Fig. 2(a)–(f) show the morphology and microstructure of sample 2 (yield 33.9 mg). As shown in Fig. 2(a) and (b), hierarchical nanostructures, which comprise of a number of flat-topped nanorods with rectangular sections of 25 × 125 nm^2 and length of about 380 nm, are vertically grown on

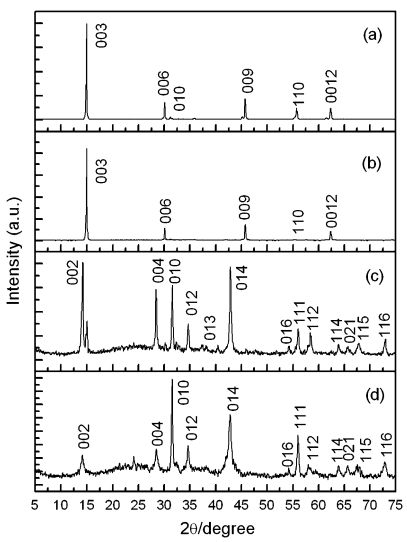

Fig. 1 Powder XRD patterns of the products prepared by chemical vapor transport with iodine: (a) 0.0, (b) 30, (c) 60, and (d) 120 mg at 750 °C for 6 h. The peaks which are not indexed in (c) can be attributed to the reflections of 3R-TaS_2. The peak which is not indexed in (d) is an unknown impurity peak with the main phase of sample 4 being the 2H-TaS_2 structure.

School of Chemistry and Chemical Engineering, Key Laboratory of Mesoscopic Chemistry of MOE, and State Key Laboratory of Coordination Chemistry, Nanjing University, Nanjing 210093, P. R. China. E-mail: wuxingca@netra.nju.edu.cn; Fax: +86-25-83317761; Tel: +86-25-83597374

† Electronic supplementary information (ESI) available: EDX spectra. See DOI: 10.1039/b905168f

 This journal is © The Royal Society of Chemistry 2009

View Online

Published on 09 June 2009 on http://pubs.rsc.org | doi:10.1039/B905168F
Downloaded by Nanjing University on 18 September 2010

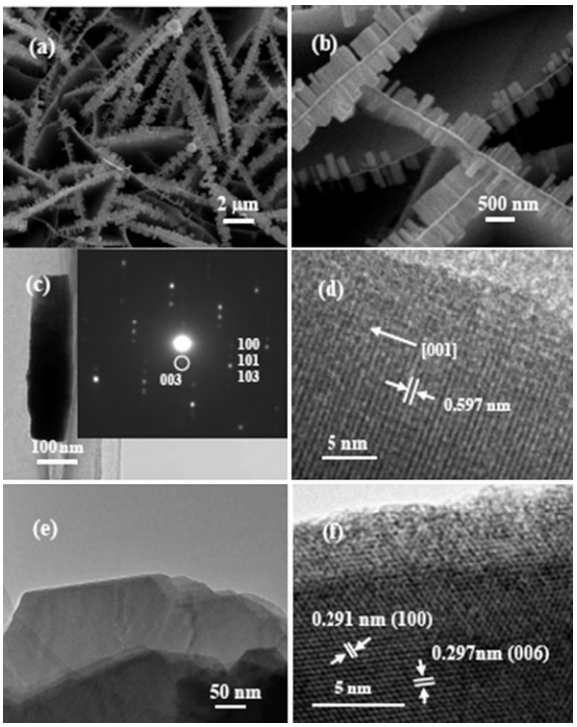

Fig. 2 Microstructures of the products prepared with 30 mg of iodine. (a, b) SEM image (overview). (c) TEM image and SAED pattern (inset) of a single nanorod. (d) HRTEM image of the nanorod in (c). (e) TEM image of a nanosheet. (f) HRTEM image of the nanosheet in (e).

the two side edges of nanosheets with a thickness of 25 nm. Fig. 2(c) displays the TEM image and SAED pattern (inset) of a single nanorod from the hierarchical nanostructures. The SAED pattern analysis supports the result of the above XRD. Fig. 2(d) shows a HRTEM image of the nanorod. The lattice spacing of 0.597 nm corresponds to the distance of the (003) plane of the 3R-TaS_2 structure, confirming [001] as the preferred growth direction for all the nanorods. Fig. 2(e) shows a TEM image of a nanosheet from the hierarchical nanostructures while Fig. 2(f) is its HRTEM image. The lattice spacings of 0.291 and 0.297 nm correspond to the distance of (100) and (006) planes of 3R-TaS_2, respectively. The EDX spectra of a single nanorod and a nanosheet reveal the presence of Ta, S and I with atomic ratios of 43.85 : 48.39 : 7.76 (= 1 : 1.10 : 0.18) and 39.87 : 53.50 : 6.63 (= 1 : 1.34 : 0.17), respectively (Fig. S1a, b) (ESI†).

Cone-topped nanorods are grown on the two side edges of nanosheets when the transport agent iodine is increased to 60 mg. The nanorods have a diameter of about 30–100 nm, and a length of about 400–1100 nm, whereas the nanosheets are about 70 nm thick, as shown in Fig. 3(a) and (b). Fig. 3(c) and (d) show the TEM and HRTEM images of a single nanorod from the hierarchical nanostructures, respectively. The lattice spacing of 0.624 nm corresponds to the distance of the (002) plane of 2H-TaS_2, confirming [001] as the preferred growth direction for all the nanorods, as above. Fig. 3(e) shows a TEM image of a nanosheet from the hierarchical nanostructures, whereas Fig. 3(f) is its HRTEM image and SAED pattern (inset). The lattice spacing of 0.262 nm

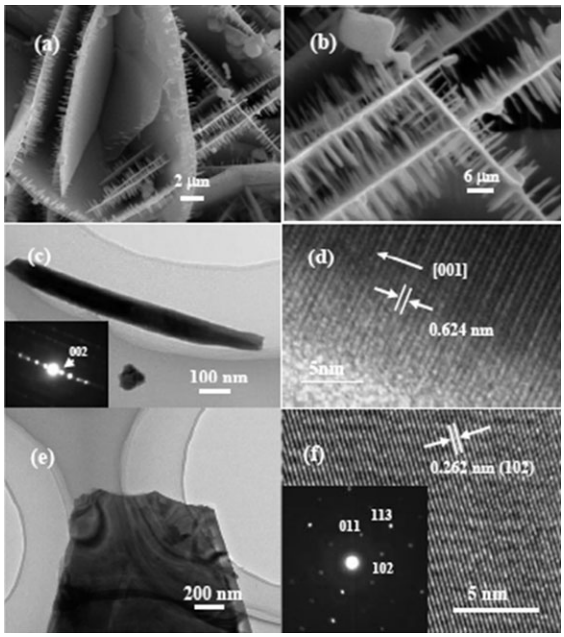

Fig. 3 Microstructures of the products prepared with 60 mg of iodine. (a, b) SEM images. (c) TEM image and SAED pattern (inset) of a single nanorod. (d) HRTEM image of the nanorod in (c). (e) TEM image of a nanosheet. (f) HRTEM image and SAED pattern (inset) of the nanosheet in (e).

corresponds to the (102) plane distance of 2H-TaS_2. The EDX analyses of a nanorod and a nanosheet demonstrate that both are composed of Ta, S and I with atomic ratios of 43.32 : 49.24 : 7.44 (= 1 : 1.14 : 0.17) and 41.35 : 52.35 : 6.30 (= 1 : 1.27 : 0.15), respectively (Fig. S2a, b) (ESI†).

Only nanosheets form and no nanorods are grown on nanosheets when the quantity of iodine is increased to 120 mg. Fig. 4(a) and (b) show the SEM image of the nanosheets. The EDX spectrum of the nanosheets shows that they consist of Ta, S and I with molar ratios of 42.99 : 51.95 : 5.06 (= 1 : 1.21 : 0.12) (Fig. S3) (ESI†). Thus the molecular formulae of the samples 2–4 can be written as $TaS_{2-x}I_y$. When the products were prepared without iodine, a mixture of hexagonal microplates and microrods were formed, as shown in Fig. 4(c) and

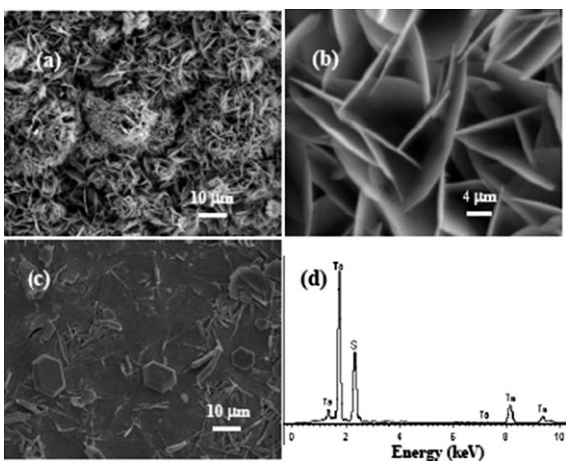

Fig. 4 (a, b) SEM image of nanosheets prepared with 120 mg of iodine. (c) SEM image of the products prepared without iodine. (d) EDX spectrum of the microplate in Fig. 4(c).

View Online

the compositions of rods and plates are close to stoichiometric TaS_2. Fig. 4(d) reveals the EDX spectrum of a microplate with Ta : S molar ratio of 33.21 : 66.79 (= 1 : 2.01). X-Ray photoelectron spectra (XPS) of samples 2–4 were measured and are shown in Fig. 5(a)–(c). Binding energies of I $3d_{5/2}$ are 619.0, 619.5 and 618.9 eV, respectively, lower than that of I_2 (I $3d_{5/2}$: 619.9 eV), and close to that of InI (I $3d_{5/2}$: 619.0 eV), so iodine is one of the compound components.

Based on the synthesis process and morphology of the products, a vapor–solid growth mechanism is proposed. First, Ta foils reacts with I_2 to form TaI_5 vapor while sulfur (bp 444.6 °C) is evaporated into gas phase. All vapors then condense on the Ta substrate to form stable $TaS_{2-x}I_y$ seeds. In the following process, TaI_5 and S in the vapor phase may have combined with the seeds to form $TaS_{2-x}I_y$ nanosheets. Because there are a lot of active positions on the edge of the nanosheets, the $TaS_{2-x}I_y$ nanorods are grown on the edge when TaI_5 reacts with S vapor continuously. Samples for magnetic measurements were prepared by carefully "peeling" off the $TaS_{2-x}I_y$ film from Ta foils. Magnetic studies were performed with a magnetometer (MPMS-XL). As shown in Fig. 6(a)–(d), the superconducting transition temperatures (T_c) of the samples 1–4 are 4.4, 5.0, 3.8 and 3.5 K, respectively, higher than those reported for bulk 2H-TaS_2 (T_c = 0.6 or 0.8 K),[15] 6R-TaS_2 nanobelts (T_c = 2.7 K),[18] and 2H-TaS_2 nanowires (T_c = 3.4 K).[19] Because 2H-TaS_2 can be produced from 1T-TaS_2 ($P\bar{3}1$, a = 3.35 and c = 5.86 Å) by annealing at 823 K and is stable at room temperature, and the slow cooling of the mixtures of the elements from the high temperatures tends to yield 3R-TaS_2,[19] the 3R-TaS_2 phase is formed easily. Friend and Yoffe concluded that the increased T_c values of materials could originate from a suppression of the periodic lattice distortion that drives charge density wave formation.[20] Therefore, the increased T_c values of the nanostructures (samples 2–4) could be attributed to the suppression of structural instability resulting from intercalation of iodine.

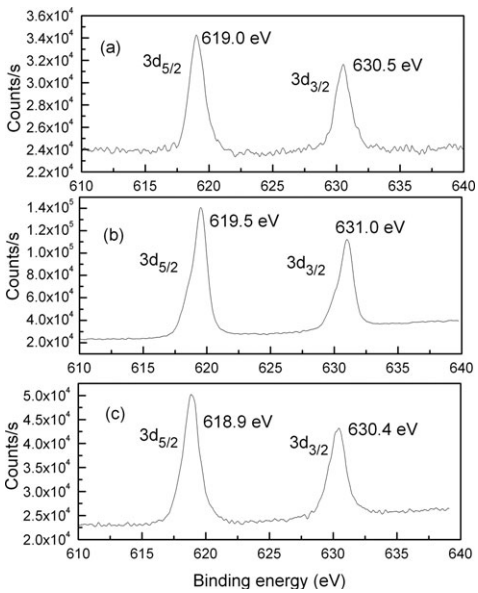

Fig. 5 I 3d binding energy spectra of the samples prepared with (a) 30, (b) 60 and (c) 120 mg of iodine, respectively.

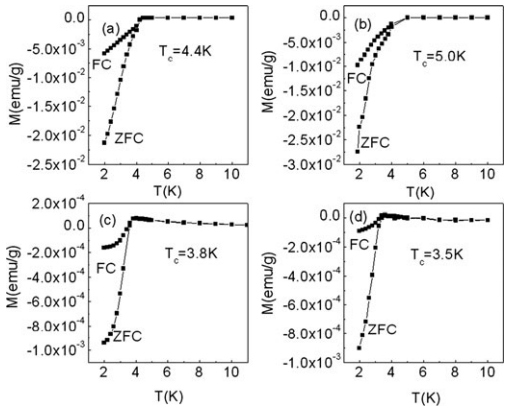

Fig. 6 DC magnetization as a function of temperature for the products prepared with (a) 0.0, (b) 30, (c) 60 and (d) 120 mg of iodine, under conditions of zero-field cooling (ZFC) and field cooling (FC) at 50 Oe.

In summary, hierarchical nanostructures of $TaS_{2-x}I_y$ have been synthesized by a facile CVT process. Iodine affects their structures, morphologies, and T_c values. This method may be used in preparing hierarchical nanostructures of other metal dichalcogenides.

The work was financially supported by the National Science Foundations of China (No. 20671050) and National Basic Research Program of China (973 Program, No. 2007CB936302).

Notes and references

1 Y. Wu, H. Yan, M. Huang, B. Messer, J. Song and P. Yang, *Chem.–Eur. J.*, 2002, **8**, 1260.
2 H. Shi, L. Qi, J. Ma and H. Cheng, *J. Am. Chem. Soc.*, 2003, **125**, 3450.
3 L. Manna, D. J. Milliron, A. Meisel, E. C. Scher and A. P. Alivisatos, *Nat. Mater.*, 2003, **2**, 382.
4 D. Zitoun, N. Pinna, N. Frolet and C. Belin, *J. Am. Chem. Soc.*, 2005, **127**, 15034.
5 K. A. Dick, K. Deppert, M. W. Larsson, T. Martensson, W. Seifert, L. R. Wallenberg and L. Samuelson, *Nat. Mater.*, 2004, **3**, 380.
6 D. Wang, F. Qian, C. Yang, Z. Zhong and C. M. Lieber, *Nano Lett.*, 2004, **4**, 871.
7 J. P. Ge, J. Wang, H. X. Zhang, X. Wang, Q. Peng and Y. D. Li, *Chem.–Eur. J.*, 2005, **11**, 1889.
8 J. Zhu, H. Peng, C. K. Chan, K. Jarausch, X. F. Zhang and Y. Cui, *Nano Lett.*, 2007, **7**, 1095.
9 M. J. Bierman, Y. K. Albert Lau and S. Jin, *Nano Lett.*, 2007, **7**, 2907.
10 D. Moore, Y. Ding and Z. L. Wang, *Angew. Chem., Int. Ed.*, 2006, **45**, 5150.
11 M. J. Bierman, Y. K. Albert Lau, A. V. Kvit, A. L. Schmitt and S. Jin, *Science*, 2008, **320**, 1060.
12 J. Zhu, H. Peng, A. F. Marshall, D. M. Barnett, W. D. Nix and Y. Cui, *Nat. Nanotechnol.*, 2008, **3**, 477.
13 K. Hayashi and A. Kawamura, *Mater. Res. Bull.*, 1986, **21**, 1405.
14 F. Jellinek, *J. Less-Common Met.*, 1962, **4**, 9.
15 A. Schlicht, M. Schwenker, W. Biberacher and A. Lerf, *J. Phys. Chem. B*, 2001, **105**, 4867.
16 M. Nath and C. N. R. Rao, *J. Am. Chem. Soc.*, 2001, **123**, 4841.
17 C. Shuffenhauer, B. A. Parkinson, N. Y. Jin-Phillipp, L. Joly-Pottuz, J. M. Martin, R. Popovitz-Biro and R. Tenne, *Small*, 2005, **1**, 1100.
18 X. C. Wu, Y. R. Tao, Y. M. Hu, Y. Song, Z. Hu, J. J. Zhu and L. Dong, *Nanotechnology*, 2006, **17**, 201.
19 C. W. Dunnill, H. K. Edwards, P. D. Brown and D. H. Gregory, *Angew. Chem., Int. Ed.*, 2006, **45**, 7060.
20 R. H. Friend and A. D. Yoffe, *Adv. Phys.*, 1987, **36**, 1.

Published on 09 June 2009 on http://pubs.rsc.org | doi:10.1039/B905168F
Downloaded by Nanjing University on 18 September 2010

 This journal is © The Royal Society of Chemistry 2009